Utilizing analytical transfer functions to gauge the effect of velocity reversals

Joaquin Garcia-Suarez[a]

[a]Civil Engineering Institute École Politechnique Fédérale de Lausanne (EPFL), Lausanne, Switzerland

1 Introduction

The analysis of wave propagation in layered media is, naturally, one of the recurrent themes in Geotechnical Earthquake Engineering and Seismology. In those cases where the intensity of the wavefront is small enough to not to trigger irreversible deformation in the medium, Linear Elastodynamics has proved itself an adequate tool to model the seismic wave propagation phenomenon. Those occasions when it fails entail large deformation of the soil, carrying irreversible changes, are usually associated to propagation in the shallow softer layers of the earth.

Assuming the earthquake source is located deep enough, the front impinges over the ground almost-vertically, as the decreasing stiffness bends the rays towards the normal of the free surface [1]. Under the assumption of one-dimensional propagation perpendicular to both the free surface and to all other internal interfaces, the different components decouple and SH, SV and P waves can be studied separately and then summed back, given that there is no mode conversion.

An approach to assess the evolution of the wavefield across the layers is the "Propagator Matrix Method" [2]. The classic Seismology textbooks [1, 3] present a general treatment for inclined SH waves and inclined P-SV waves. No inclination is considered here, thus the expressions that will appear represent a particular case. An approach for the 1D case, often used in geotechnical engineering, is presented in [4].

There is no definitive understanding over the effect of each layer over the final global transfer function [5]. In particular, the effect of so-called velocity reversals is still inquired nowadays. The term "velocity reversal" refers to intermediate layers that break the monotonicity of the stiffness distribution along depth: in usual circumstances, one encounters that the wave velocity increases the deeper the layer is (this is not only due to different geological conditions, but also to the cumulative effect of overburden pressure), a velocity reversal is a layer that does not abide by this trend, as it is softer than both the layer immediately

above and the one immediately below. One could think of it as a soft inclusion in a stiff medium.

Yagoda-Biran, Kerpel and Kamai [6] carried out a thorough parametric investigation on the effect of the velocity reversals over the displacement-to-amplitude transfer function of a two-layer system over a half-space. Chiefly, they found that:

1. The amplitude of the tranfer function at the first resonance peak scales proportionally to the impedance ratio between reversal and half-space in a 3-layer system (bottom layer being the half-space).

2. A criterion to ensure minor influence of reversals can be furnished for such systems.

This work tackles the same problem but from a purely analytical basis. Utilizing the exact expression of the transfer function (which can be obtained from the propagator matrices), an argument based on relative magnitude of different terms *during the (first) resonance peak* will be leveled.

All the results are made available to the research community: the Mathematica notebook utilized to carry out the computations can be found on GitHub (see Supplementary Material).

2 Scaling of fundamental mode amplitude

The transfer function for a system made up of 2 layers overlying a half-space are given next. See the appendix for derivation of these results. The width, shear modulus, density and shear-wave velocity of the top (bottom) layer are h_1, μ_1, ρ_1, V_{s1} (h_2, μ_2, ρ_2, V_{s2}). The circular frequency of the wave is denoted by ω.

The expression studied by Madera [7] gives the displacement-displacement transfer function:

$$\mathsf{TF}(\omega)^{-1} = \frac{\hat{u}_{top}}{\hat{u}_{half}} = \cos(r_1)\cos(r_2) - Z_1 \sin(r_1)\cos(r_2)\,, \tag{1}$$

where $r_1 = h_1\omega/V_{s1}$, $r_2 = h_2\omega/V_{s2}$, $\hat{u}_{top}$ is the spectral amplitude of the displacement at the ground level while $\hat{u}_{half}$ is at the interface between the bottom layer and the half-space, $Z_1 = (\rho_1\mu_1/\rho_2\mu_2)^{1/2}$ is the impedance contrast between first and second layer.
Likewise, the displacement-amplitude transfer function is:

$$\begin{aligned}2\mathrm{TF}(\omega)^{-1} = \frac{\hat{u}_{top}}{\acute{S}} = \cos(r_1)\cos(r_2) - Z_1 \sin(r_1)\cos(r_2) \\ + \mathrm{i}Z_1 Z_2 \sin(r_1)\cos(r_2) + \mathrm{i}Z_2 \sin(r_2)\cos(r_1)\,,\end{aligned} \tag{2}$$

where $\acute{S}$ refers to the impinging S-wave amplitude coming from the half-space, while $Z_2 = (\rho_2\mu_2/\rho_{half}\mu_{half})^{1/2}$ is the impedance contrast between the second layer and the half-space.

Let us state the obvious relation between the two transfer functions:

$$\frac{2}{\mathrm{TF}} = \frac{1}{\mathsf{TF}} + \mathrm{i}Z_1 Z_2 \sin(r_1)\cos(r_2) + \mathrm{i}Z_2 \sin(r_2)\cos(r_1)\,. \tag{3}$$

The consequential effect of the presence of the velocity reversal (second layer) is that $Z_1 > 1$, whereas $Z_2 < 1$. See how it follows that $Z_2/Z_1 < Z_2$ and hence we may assume $Z_2/Z_1 << 1$ for as long as there is a velocity reversal and a bedrock halfspace stiffer than the upper layers. The possibility of exploiting Z_2/Z_1 as if it was a small parameter in the expression allows to pursue the following argumentation.

Let us focus on $2\mathrm{TF}^{-1}/Z_1$, which, from eq. (2), is

$$\begin{aligned}\frac{2\mathrm{TF}(\omega)^{-1}}{Z_1} &= \frac{\cos(r_1)\cos(r_2)}{Z_1} - \sin(r_1)\cos(r_2) \\ &\quad + \mathrm{i}\frac{Z_2}{Z_1}\left(\cos(r_1)\sin(r_2) + Z_1\cos(r_2)\sin(r_1)\right)\,, \end{aligned} \tag{4a}$$

let us call $\varepsilon = Z_2/Z_1$ and assume $\varepsilon \ll 1$, so

$$\begin{aligned}&= \frac{\cos(r_1)\cos(r_2)}{Z_1} - \sin(r_1)\cos(r_2) \\ &\quad + \varepsilon\mathrm{i}\left(\sin(r_1)\cos(r_2) + Z_1\sin(r_2)\cos(r_1)\right)\,, \end{aligned} \tag{4b}$$

and, see eq. (3), recognize the first two addens as TF^{-1}/Z_1,

$$= \mathsf{TF}^{-1}/Z_1 + \mathcal{O}\left(\varepsilon\right)\,. \tag{4c}$$

This last result means that the displacement-to-amplitude transfer function, TF, can be thought to be the displacement-to-displacement transfer function plus a small correction term order ε. In particular, see that, in absence of material damping dissipation, $|\mathsf{TF}^{-1}| \approx 0$ during resonance (resonance frequency $\omega = \omega_1$), so $\mathrm{TF}^{-1}/Z_1|_{\omega=\omega_1} = \mathcal{O}(\varepsilon)$, the residual amplitude (which is small but remains finite even in the case of no material damping) corresponds to the amplitude of the fundamental resonance mode, and its boundedness (unlike in the case of the other transfer function) can be interpreted as a consequence of the radiational damping, which is acounted for by the imaginary addends in eq. (2), absent from eq. (1).

Another remarkable consequence of eq. (3) is that, since the resonance peak for both TF and TF coincides, the resonance frequency can be thought as independent of the properties of the half-space; in other words, the presence of the reversal decouples the resonance of the top strata from the features of the half-space.

Let us unpack the amplitude at resonance next. One can estimate both upper and lower bounds of the amplitude during resonance. First, the lower bound:

$$|\mathrm{TF}(\omega = \omega_1)| \approx \frac{2}{|Z_1 Z_2 \cos(r_1)\sin(r_2) + Z_2\cos(r_2)\sin(r_1)|_{\omega=\omega_1}} \tag{5a}$$

since both since and cosine are bounded by 1,

$$\geq \frac{2}{Z_1 Z_2 + Z_2} = \frac{2}{Z_1 Z_2 (1 + \underbrace{1/Z_1}_{<1})} \approx \frac{2}{Z_1 Z_2} = 2\sqrt{\frac{\rho_{half}\mu_{half}}{\rho_1 \mu_1}}\,. \tag{5b}$$

See that this lower bound depends on the properties of the upper layer yet not on the reversal's, even though the result is derived exploiting its presence.

Additionally, an upper bound for the amplitude at resonance can also be argued:

$$|\mathrm{TF}(\omega = \omega_1)| \approx \frac{2}{|Z_1 Z_2 \cos(r_1)\sin(r_2) + Z_2 \cos(r_2)\sin(r_1)|_{\omega=\omega_1}} \tag{6a}$$

$$= \frac{2/Z_2}{|Z_1 \cos(r_1)\sin(r_2) + \cos(r_2)\sin(r_1)|_{\omega=\omega_1}}\,, \tag{6b}$$

the first addend in the numerator can be greater than one, unlike the second addend; if we want to minimize the denominator this term must be deactivated and such thing would happen when $r_2 \ll 1$, thus $\sin(r_2) \approx 0$, while $\cos(r_2) \approx 1$, so

$$\leq \frac{2/Z_2}{|\sin(r_1)|}\,, \tag{6c}$$

moreover, assuming that the denominator is close to 1 in this situation, finally yields

$$\approx \frac{2}{Z_2} = 2\sqrt{\frac{\rho_{half}\mu_{half}}{\rho_2 \mu_2}}\,. \tag{6d}$$

The properties of the upper layer do not appear in the formula of the upper bound.

2.1 Verification

In order to verify the results we resort to computing numerical transfer functions and comparing them to eq. (5b) and eq. (6d).

The set of profiles to be analyzed is the one presented in [6]: there are a total of 140 profiles, the upper layer shear-wave velocity ranging from 400 to 800 m/s, in increments of 100 m/s, while the lower layer shear-wave velocity ranges between 300 and 800 in increments of 50 m/s; only the combinations that yield $V_{s1} \geq V_{s2}$ are considered. The density in each layer is assumed to be a linear function of the wave velocity in the layer defined by assigning density $1800\,\mathrm{kg/m^3}$ when the velocity is 200m/s and $2100\,\mathrm{kg/m^3}$ when the velocity is 900 m/s. The thickness of the two layers sum up to 50 m in all cases, the breakdown being defined by $h_1/h_2 = 10/40,\ 20/30,\ 30/20,\ 40/10$.

The damping factor used in [6] was 10% across all layers; the prior derivation of the bounds did not include the damping for the sake of clarity, but it can be added on the derivation easily, just consider that $|\mathsf{TF}(\omega = \omega_1)^{-1}| \approx \pi/4\delta_d$ [8]

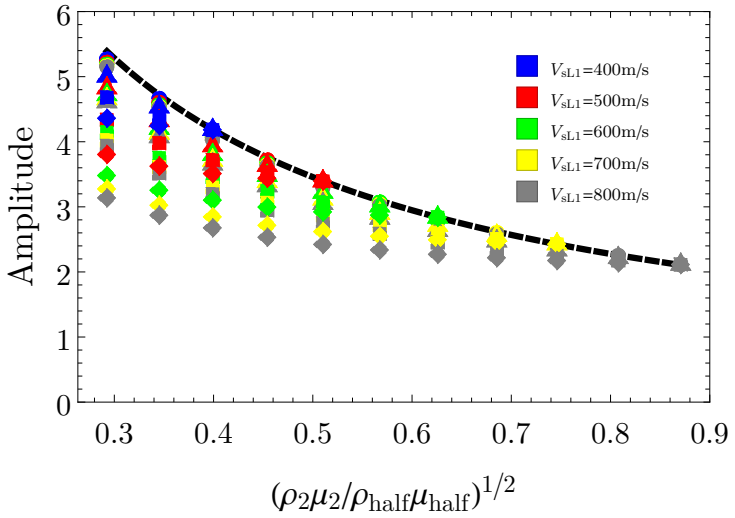

Figure 1: Verification upper bound: amplitude of first resonance peaks as a function of impedance contrast bottom stratum (reversal) v. half-space, for different combinations of parameters. Markers relate to thickness ratios: circles, 10/40; triangles, 20/30; squares, 30/20; and diamonds, 40/10.

(instead of zero). Thus, the expression of the lower bound, originally eq. (5b) that includes material damping is

$$|\text{TF}(\omega = \omega_1)| \geq \frac{2}{\frac{\pi}{4}\delta_d + \sqrt{\frac{\rho_1\mu_1}{\rho_{half}\mu_{half}}}} \tag{7a}$$

while the upper bound, after updating eq. (6d) in similar fashion,

$$|\text{TF}(\omega = \omega_1)| \leq \frac{2}{\frac{\pi}{4}\delta_d + \sqrt{\frac{\rho_2\mu_2}{\rho_{half}\mu_{half}}}}\,. \tag{7b}$$

One acknowledges that the numerical results lie below eq. (7b), see Figure 1, and over eq. (7a), Figure 2.

Since the results lie between an upper bound, that depends only on the properties of the half-space and the first layer's, and a lower bound that depends only on the properties of the half-space and the second layer's, it is logical to think that the actual amplitudes must depend on some function of the three (upper, lower and half-space). In [6], the authors put forward the idea of homogenizing the two layers into an equivalent one with velocity given by the "time-averaged velocity" (harmonic mean), then compared its resonance amplitude to the one of the stratified model, obtaining remarkable agreement (even though the harmonic mean is known not to be optimal to homogeneize a continuum that undergoes fundamental resonance [9]).

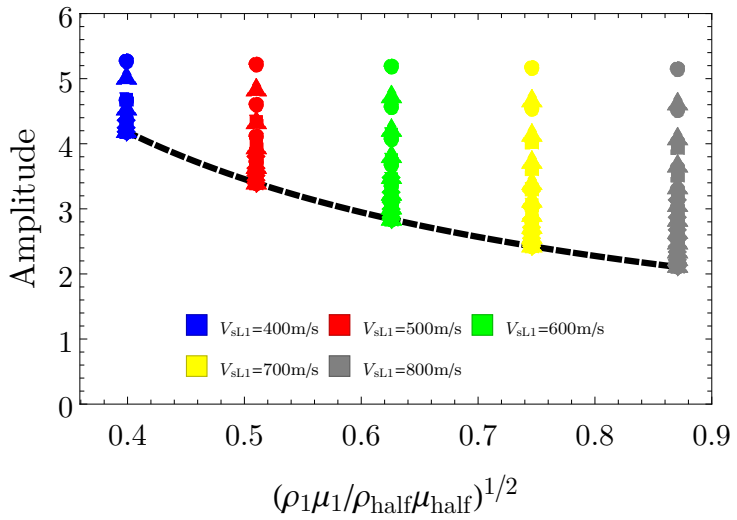

Figure 2: Verification lower bound: amplitude of first resonance peaks as a function of impedance contrast top stratum v. half-space, for different combinations of parameters. Markers relate to thickness ratios: circles, 10/40; triangles, 20/30; squares, 30/20; and diamonds, 40/10.

3 Reversals in more complex lithography: no easy assessment

The prospect for a definition of small parameter and for dividing the terms in clear-cut groups of different magnitude vanishes when moving to more complex scenarios. Recall that the small parameter was the key to the split of the transfer function into two parts, one controlling the position of the fundamental mode, and the second one controlling its amplitude. This feature being absent leaves no room for a reasoning analogous to the one carried out for the 2-layer one.

Let us illustrate this situation regarding at a 3-layer site overlying a half-space. In such a scenario the reversal can be located either between the first and the third layer ($Z_1 > 1$), or between the second and the half-space ($Z_2 > 1$).

The 3-layer-over-halfspace transfer function is

$$\begin{aligned}2\mathrm{TF}(\omega)^{-1} = \cos(r_1)\cos(r_2)\cos(r_3) &- Z_1\sin(r_1)\sin(r_2)\cos(r_3)\\ &- Z_1Z_2\sin(r_1)\cos(r_2)\sin(r_3)\\ &- Z_2\cos(r_1)\sin(r_2)\sin(r_3)\\ &- \mathrm{i}Z_1Z_2Z_3\sin(r_1)\cos(r_2)\cos(r_3)\\ &- \mathrm{i}Z_2Z_3\cos(r_1)\sin(r_2)\cos(r_3)\\ &- \mathrm{i}Z_3\cos(r_1)\cos(r_2)\sin(r_3)\\ &+ \mathrm{i}Z_1Z_3\sin(r_1)\sin(r_2)\sin(r_3)\,, \qquad (8)\end{aligned}$$

See how the split on the grounds of the assumption of one velocity reversal in either position is not straightforward, as one can not trace a division in terms of magnitude the way it was done in the previous section, which may have enabled pursuing a similar argumentation.

4 Final Remarks

An analytical interpretation of the results presented in [6] has been laid out in the text. The key step in the derivation was to leverage the presence of a small parameter in order to split the displacement-amplitude transfer function into a portion with larger magnitude that still vanishes during resonance (identified with the displacement-displacement transfer function) and small-magnitude term representing the radiational damping which controls the amplitude during resonance.

The validity of the assumption, upon which the rest of the results rest, has been accredited with a derivation of an upper and a lower bound of the amplitude, which naturally follows from the simplified expressions. These bounds have also been verified later via comparison to numerical results obtained through the conventional approach (evaluating propagator matrices).

In summary:

- In the 2-layer case, the presence of the reversal renders the fundamental resonance frequency independent of the material properties of the half-space.
- The effect of velocity reversals over the dynamic response can be described precisely in the 2-layer case, but doing so is not straightforward when it comes to sites with more than two layers overlying a rigid half-space.

This work also proves the possibility of extracting useful general insights by working directly in analytical terms.

Let us mention, just like it was done in the original paper [6], that the results are circumscribed to small-intensity seismic-wave propagation owing to the linearity assumption. A further study that could account for the effect of large magnitude earthquakes on the soil must take into account non-linear material response necessarily [10].

Acknowledgements

The author is grateful to Alexey Popkov (`github.com/AlexeyPopkov`), since code developed by him has been used to generate the plots.

Supplementary Material

A *Mathematica* notebook titled `Reversals` containing the evaluation of the results in this manuscript can be found in the author's Github page: `github.com/jgarciasuarez`.

References

[1] Keiiti Aki and Paul G. Richards. *Quantitative seismology*. University Science Books, Sausalito, California, 2nd ed edition, 2002.

[2] Freeman Gilbert and George E. Backus. Propagator matrices in elastic wave and vibration problems. *Geophysics*, 31(2):326–332, April 1966.

[3] Ari Ben-Menahem and Sarva Jit Singh. *Seismic Waves and Sources*. Springer New York, New York, NY, 1981.

[4] Steven Lawrence Kramer. *Geotechnical earthquake engineering*. Prentice-Hall international series in civil engineering and engineering mechanics. Prentice Hall, Upper Saddle River, N.J, 1996.

[5] M Pehlivan, YMA Hashash, JA Harmon, EM Rathje, JP Stewart, SJ Silva, KW Campbell, and S Nikolaou. Influence of shear wave velocity reversals on one-dimensional site response of spatially varied profiles. 2015.

[6] Gony Yagoda-Biran, Bibi Kerpel, and Ronnie Kamai. Never Fear Velocity Reversals. *Bulletin of the Seismological Society of America*, page ssabull;0120170028v1, July 2017.

[7] Gregory A Madera. Fundamental period and amplification of peak acceleration in layered systems, mass. research report r 70–37. 1970.

[8] Jose M Roesset. Soil amplification of earthquakes. *Numerical methods in geotechnical engineering*, pages 639–682, 1977.

[9] Joaquin Garcia-Suarez, Domniki Asimaki, and Elnaz E Seylabi. Geometrical optics applied to 1d site response of inhomogeneous soil deposits, Feb 2020.

[10] Mehmet Darendeli. *Development of New Family of Normalized Modulus Reduction and Material Damping Curves*. PhD thesis, University of Texas, Austin, 12 2001.

[11] H. Kawase, F. J. Sanchez-Sesma, and S. Matsushima. The Optimal Use of Horizontal-to-Vertical Spectral Ratios of Earthquake Motions for Velocity Inversions Based on Diffuse-Field Theory for Plane Waves. *Bulletin of the Seismological Society of America*, 101(5):2001–2014, October 2011.

A Review of matrix propagator methods and exact expression for transfer functions in of two-layer medium

A propagator matrix is assigned to each soil portion, its entries depending on the mechanical properties of the material of the layer as well as on the wavelength of the propagating plane wave, then these matrices are shown to relate stresses and displacements in opposite ends of the layer.

One chief application of this matrix method is to obtain "transfer functions" relating the displacement amplitude at the free surface to either the displacement at a lower level or to the amplitude of a impinging wave arising from half-space and reaching the upper strata and the free surface.

Once our assumptions have been laid out, consider S waves propagating normally to layers and ground interfaces, eliciting a linear-elastic response in the soil. As it is customary, it is assumed that either the Fourier transform has been applied to the equations of the problem or a steady-state plane-wave solution has been assumed, thus the results are given in the frequency domain. The method considers balance of linear momentum (equilibrium) and the constitutive relation (relation stress-strain). Under the 1D assumption, frequency-domain, for S waves, these equations in matrix form read as:

$$\frac{d\boldsymbol{f}}{dz} = \frac{d}{dz}\begin{bmatrix}\hat{u}\\ \hat{\tau}_{xz}\end{bmatrix} = \begin{bmatrix}0 & 1/\mu_k\\ -\rho_k\omega^2 & 0\end{bmatrix}\begin{bmatrix}\hat{u}\\ \hat{\tau}_{xz}\end{bmatrix} = \boldsymbol{A}_k\boldsymbol{f}(z)\,, \tag{9}$$

where z is the vertical coordinate, see **??**, $\hat{u}$ represents the Fourier-amplitude (frequency-domain amplitude) of the horizontal displacement, $\hat{\tau}_{xz}$ is the amplitude of the shear stresses, μ_k and ρ_k refer respectively to the shear modulus and the density of the soil, and ω is the circular frequency of the propagating wave. Later on, we will also discuss the effect of hysteretic damping in the soil, hence we will use the symbol $\delta_{d,k}$ to refer to the damping coefficient of the k-th layer. We shall use $\delta_{d,k} = \delta_d = 0.10$ for all layers. Appealing to the Equivalence Principle [3], introducing this dissipative behavior in the material frequency-domain responseis euivalent to substituting the real shear modulus μ_k by a complex one given by $\mu_k(1 + \mathrm{i}\delta_{d,k})$. See also that sometimes the imaginary part of the shear modulus (loss modulus) is expressed as $2\mu_k\delta_d$, in particular in [6], so what amounts to a damping value of a 5% is 10% in the formulation herein chosen. This is the damping value used for all layers.

We assume that conditions at the top of the layer are given by $\boldsymbol{f}(z = z_{k-1})$. The vector $\boldsymbol{f}$ is called the motion-stress vector, the matrix $\boldsymbol{A}_k$ is referred as the

k-th layer matrix. For a given frequency, the matrix layer is a constant within the layer as mechanical properties remain constant themselves.

The solution for eq. (9) can be written as

$$\boldsymbol{f}(z) = \boldsymbol{P}(z, z_{k-1})\boldsymbol{f}(z = z_{k-1}) \quad \text{, for} \quad z_{k-1} \leq z \leq z_k \,. \tag{10}$$

The propagator matrix of the k-th layer, $\boldsymbol{P}(z, z_{k-1})$, is given by

$$\boldsymbol{P}(z, z_{k-1}) = \begin{bmatrix} \cosh(\nu_k(z - z_{k-1})) & (\mu_k\nu_k)^{-1}\sinh(\nu_k(z - z_{k-1})) \\ \mu_k\nu_k \sinh(\nu_k(z - z_{k-1})) & \cosh(\nu_k(z - z_{k-1})) \end{bmatrix}, \tag{11}$$

is the propagator matrix for the k-th layer: therein, it appears $\pm\nu = \pm\sqrt{-\rho_k\omega^2/\mu_k}$ which are the eigenvalues of the layer matrix $\boldsymbol{A}_k$, recall eq. (9).

A.1 Cumulative Propagator

By recursion, the motion-stress vector at any depth (say, somewhere within the k-th layer) can be written in terms of the one of the free-surface ($z = z_0 = 0$) as

$$\begin{aligned} \boldsymbol{f}(z) &= \boldsymbol{P}(z, z = 0)\boldsymbol{f}(0) && \text{(12a)} \\ &= (\boldsymbol{P}(z, z_{k-1})\boldsymbol{P}(z_{k-1}, z_{k-2}) \ldots \boldsymbol{P}(z_2, z_1)\boldsymbol{P}(z_1, z_0))\, \boldsymbol{f}(0) && \text{(12b)} \\ &= \boldsymbol{P}(z, z_{k-1}) \left[\prod_{l=1}^{k-1} \boldsymbol{P}(z_l, z_{l-1})\right] \boldsymbol{f}(0)\,, && \text{(12c)} \end{aligned}$$

thus the product of relation between the vectors at any two interfaces through a cumulative propagator can be expressed as a product of elemental single-layer propagator matrices.

A.2 Relation to Transfer functions

A.2.1 Displacement-displacement

The stress-free condition translates into a zero entry of the motion-stress vector at $z = z_0 = 0$:

$$\boldsymbol{f}(0) = [\hat{u}_{top} \quad 0]^\top \,. \tag{13}$$

This means that the relation between the displacement amplitude at the free-surface, $\hat{u}_{top}$ and the displacement at any other interface, say, the k-th one, comes given by

$$\boldsymbol{f}(z = z_k) = \begin{bmatrix} \hat{u} \\ \hat{\tau}_{xz} \end{bmatrix}_{z=z_k} = \boldsymbol{P}(z_k, 0) \begin{bmatrix} \hat{u}_{top} \\ 0 \end{bmatrix} \rightarrow \mathsf{TF}(\omega) = \frac{\hat{u}_{top}}{\hat{u}(z = z_k)} = \frac{1}{P_{11}(z_k, 0)} \,. \tag{14}$$

A.2.2 Displacement-impinging amplitude

Let us focus on the last layer overlying the half-space [6, 11]. The displacement at the base of the last layer is equal to the one at the top of the half-space, which in turn is given by the superposition of the impinging wave and the transmitted back into the half-space after traversing the upper layered soil back and forth. Following the traditional seismological notation, $\acute{S}$ represents the upward-going wave amplitude, while $\grave{S}$, the down-going one. Thus, we can write the base-to-top relation as

$$\boldsymbol{f}(z = z_k) = \begin{bmatrix} \hat{u} \\ \hat{\tau}_{xz} \end{bmatrix}_{z=z_k} = \begin{bmatrix} \grave{S} + \acute{S} \\ \mu_{half}\mathrm{ik}(\grave{S} - \acute{S}) \end{bmatrix}_{z=z_k} = \boldsymbol{P}(z_k, z_0) \begin{bmatrix} \hat{u}_{top} \\ 0 \end{bmatrix} = \begin{bmatrix} P_{11}\hat{u}_{top} \\ P_{21}\hat{u}_{top} \end{bmatrix}, \tag{15}$$

thus the ratio $\hat{u}_{top}/\acute{S}$ can be written as

$$\mathrm{TF}(\omega) = \frac{\hat{u}_{top}}{\acute{S}} = \frac{2}{P_{11} - \mathrm{i}\frac{P_{21}}{\omega\sqrt{\rho_{half}\mu_{half}}}}. \tag{16}$$

B Transfer Function plots

The transfer functions are evaluated from the analytical solution eq. (2) ("Analytical"), following the methodology in [1] ("A&R") and the one in [4] ("Kramer"). The symbol $\acute{S}$ is substituted by S_i.

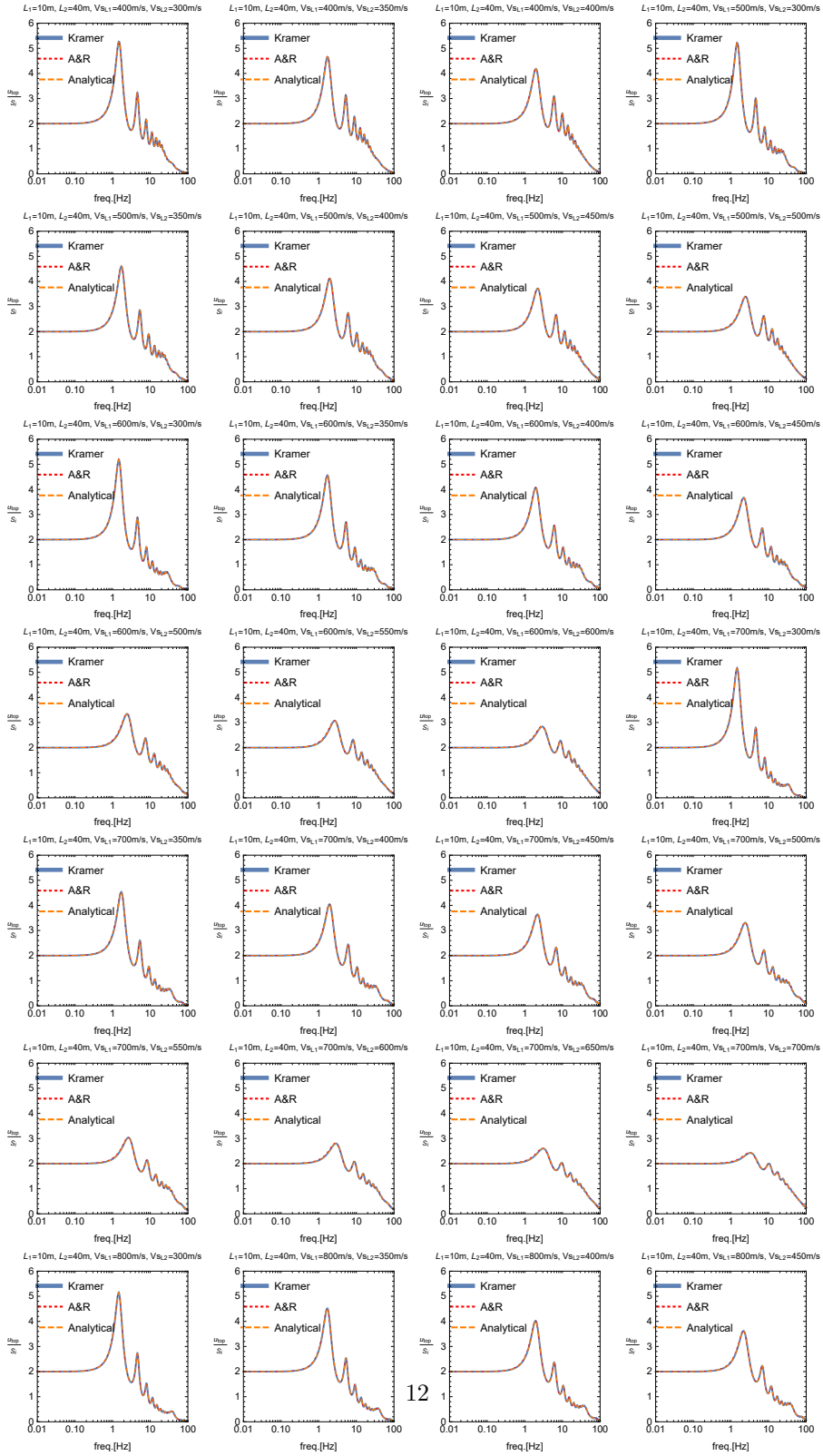
L_1=10m, L_2=40m, Vs_{L1}=400m/s, Vs_{L2}=300m/s
L_1=10m, L_2=40m, Vs_{L1}=400m/s, Vs_{L2}=350m/s
L_1=10m, L_2=40m, Vs_{L1}=400m/s, Vs_{L2}=400m/s
L_1=10m, L_2=40m, Vs_{L1}=500m/s, Vs_{L2}=300m/s
L_1=10m, L_2=40m, Vs_{L1}=500m/s, Vs_{L2}=350m/s
L_1=10m, L_2=40m, Vs_{L1}=500m/s, Vs_{L2}=400m/s
L_1=10m, L_2=40m, Vs_{L1}=500m/s, Vs_{L2}=450m/s
L_1=10m, L_2=40m, Vs_{L1}=500m/s, Vs_{L2}=500m/s
L_1=10m, L_2=40m, Vs_{L1}=600m/s, Vs_{L2}=300m/s
L_1=10m, L_2=40m, Vs_{L1}=600m/s, Vs_{L2}=350m/s
L_1=10m, L_2=40m, Vs_{L1}=600m/s, Vs_{L2}=400m/s
L_1=10m, L_2=40m, Vs_{L1}=600m/s, Vs_{L2}=450m/s
L_1=10m, L_2=40m, Vs_{L1}=600m/s, Vs_{L2}=500m/s
L_1=10m, L_2=40m, Vs_{L1}=600m/s, Vs_{L2}=550m/s
L_1=10m, L_2=40m, Vs_{L1}=600m/s, Vs_{L2}=600m/s
L_1=10m, L_2=40m, Vs_{L1}=700m/s, Vs_{L2}=300m/s
L_1=10m, L_2=40m, Vs_{L1}=700m/s, Vs_{L2}=350m/s
L_1=10m, L_2=40m, Vs_{L1}=700m/s, Vs_{L2}=400m/s
L_1=10m, L_2=40m, Vs_{L1}=700m/s, Vs_{L2}=450m/s
L_1=10m, L_2=40m, Vs_{L1}=700m/s, Vs_{L2}=500m/s
L_1=10m, L_2=40m, Vs_{L1}=700m/s, Vs_{L2}=550m/s
L_1=10m, L_2=40m, Vs_{L1}=700m/s, Vs_{L2}=600m/s
L_1=10m, L_2=40m, Vs_{L1}=700m/s, Vs_{L2}=650m/s
L_1=10m, L_2=40m, Vs_{L1}=700m/s, Vs_{L2}=700m/s
L_1=10m, L_2=40m, Vs_{L1}=800m/s, Vs_{L2}=300m/s
L_1=10m, L_2=40m, Vs_{L1}=800m/s, Vs_{L2}=350m/s
L_1=10m, L_2=40m, Vs_{L1}=800m/s, Vs_{L2}=400m/s
L_1=10m, L_2=40m, Vs_{L1}=800m/s, Vs_{L2}=450m/s
Kramer
A&R
Analytical
freq.[Hz]

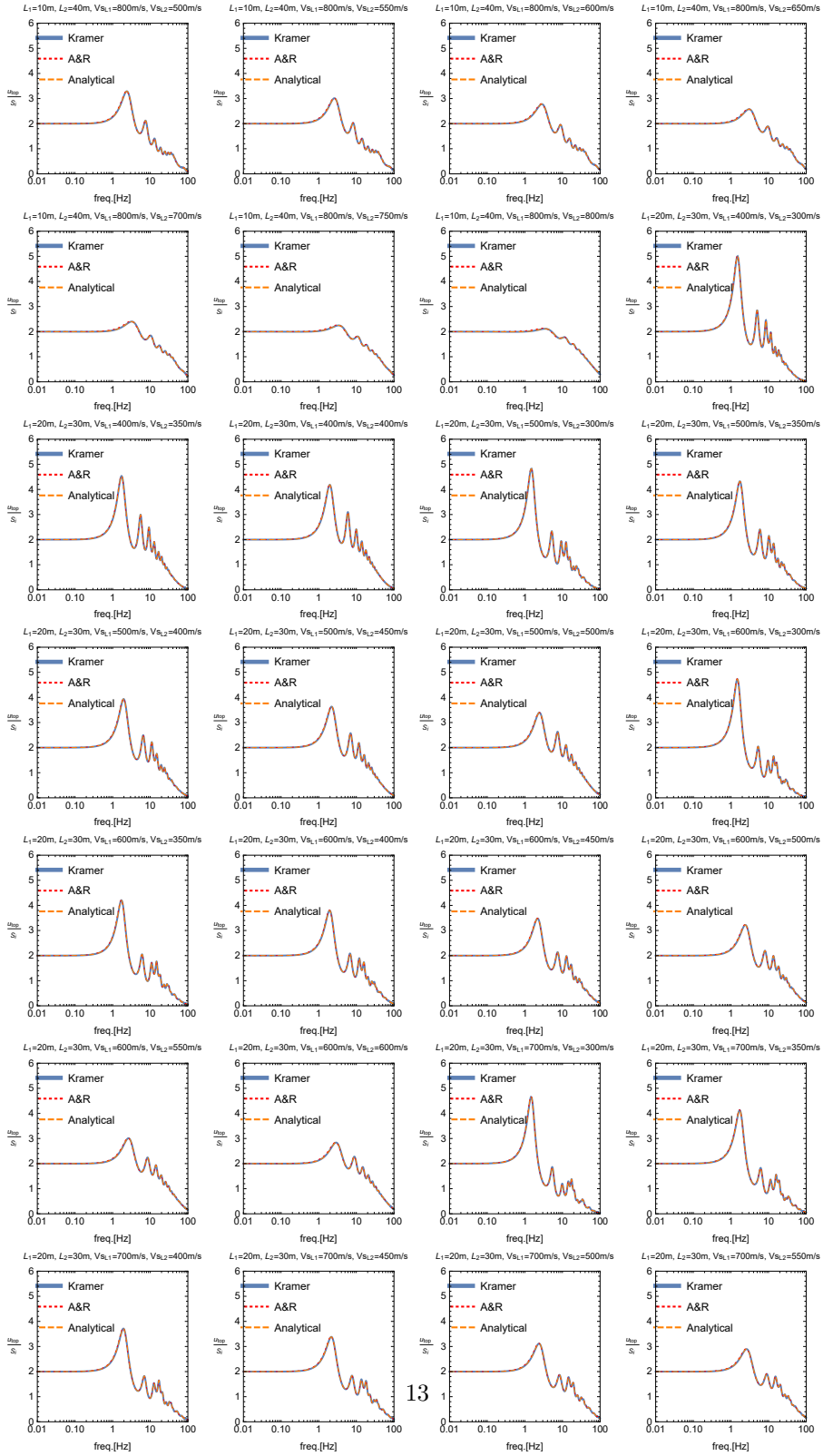
L_1=10m, L_2=40m, Vs_{L1}=800m/s, Vs_{L2}=500m/s
L_1=10m, L_2=40m, Vs_{L1}=800m/s, Vs_{L2}=550m/s
L_1=10m, L_2=40m, Vs_{L1}=800m/s, Vs_{L2}=600m/s
L_1=10m, L_2=40m, Vs_{L1}=800m/s, Vs_{L2}=650m/s
L_1=10m, L_2=40m, Vs_{L1}=800m/s, Vs_{L2}=700m/s
L_1=10m, L_2=40m, Vs_{L1}=800m/s, Vs_{L2}=750m/s
L_1=10m, L_2=40m, Vs_{L1}=800m/s, Vs_{L2}=800m/s
L_1=20m, L_2=30m, Vs_{L1}=400m/s, Vs_{L2}=300m/s
L_1=20m, L_2=30m, Vs_{L1}=400m/s, Vs_{L2}=350m/s
L_1=20m, L_2=30m, Vs_{L1}=400m/s, Vs_{L2}=400m/s
L_1=20m, L_2=30m, Vs_{L1}=500m/s, Vs_{L2}=300m/s
L_1=20m, L_2=30m, Vs_{L1}=500m/s, Vs_{L2}=350m/s
L_1=20m, L_2=30m, Vs_{L1}=500m/s, Vs_{L2}=400m/s
L_1=20m, L_2=30m, Vs_{L1}=500m/s, Vs_{L2}=450m/s
L_1=20m, L_2=30m, Vs_{L1}=500m/s, Vs_{L2}=500m/s
L_1=20m, L_2=30m, Vs_{L1}=600m/s, Vs_{L2}=300m/s
L_1=20m, L_2=30m, Vs_{L1}=600m/s, Vs_{L2}=350m/s
L_1=20m, L_2=30m, Vs_{L1}=600m/s, Vs_{L2}=400m/s
L_1=20m, L_2=30m, Vs_{L1}=600m/s, Vs_{L2}=450m/s
L_1=20m, L_2=30m, Vs_{L1}=600m/s, Vs_{L2}=500m/s
L_1=20m, L_2=30m, Vs_{L1}=600m/s, Vs_{L2}=550m/s
L_1=20m, L_2=30m, Vs_{L1}=600m/s, Vs_{L2}=600m/s
L_1=20m, L_2=30m, Vs_{L1}=700m/s, Vs_{L2}=300m/s
L_1=20m, L_2=30m, Vs_{L1}=700m/s, Vs_{L2}=350m/s
L_1=20m, L_2=30m, Vs_{L1}=700m/s, Vs_{L2}=400m/s
L_1=20m, L_2=30m, Vs_{L1}=700m/s, Vs_{L2}=450m/s
L_1=20m, L_2=30m, Vs_{L1}=700m/s, Vs_{L2}=500m/s
L_1=20m, L_2=30m, Vs_{L1}=700m/s, Vs_{L2}=550m/s
Kramer
A&R
Analytical
freq.[Hz]

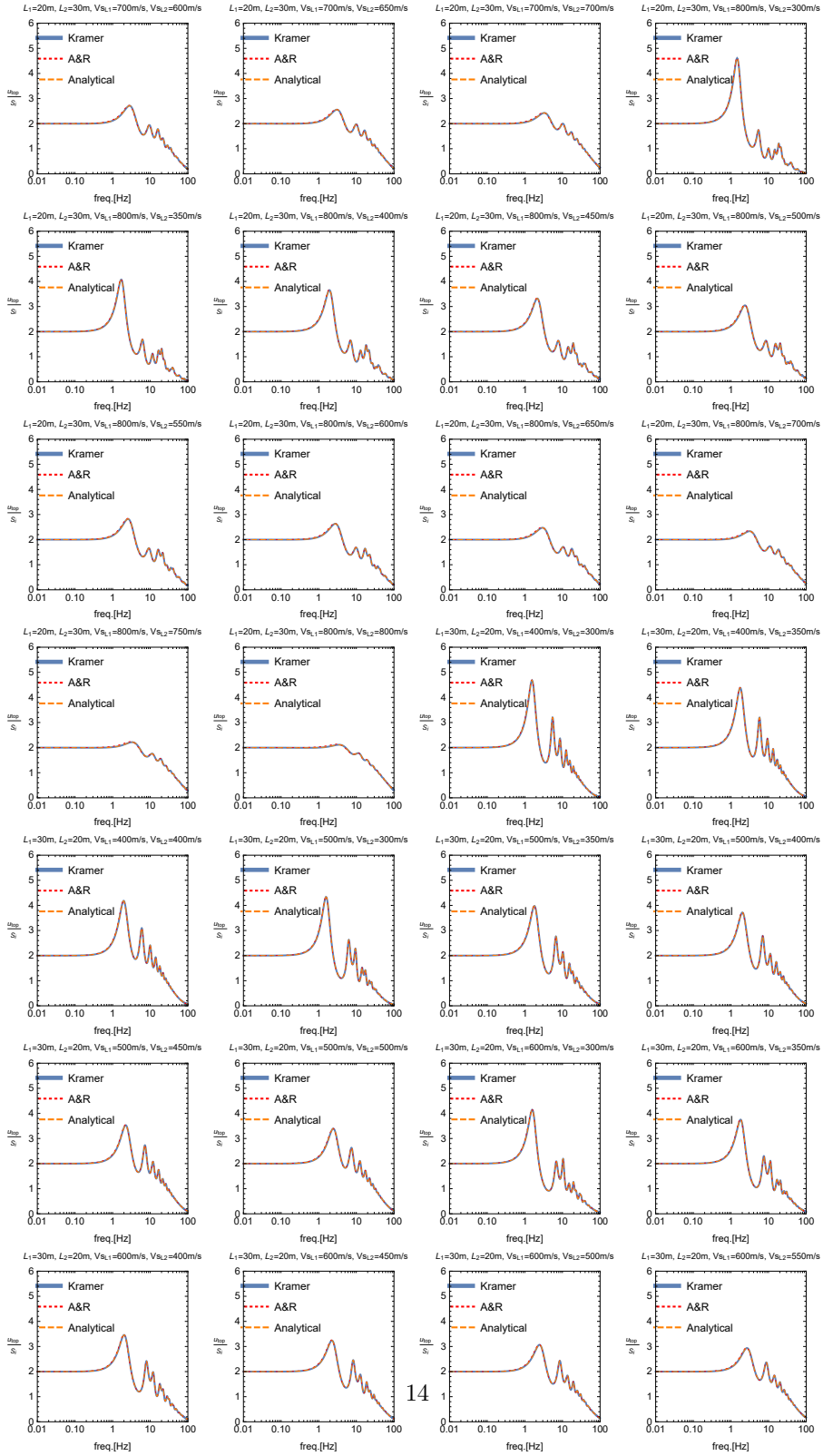
L_1=20m, L_2=30m, Vs_{L1}=700m/s, Vs_{L2}=600m/s
L_1=20m, L_2=30m, Vs_{L1}=700m/s, Vs_{L2}=650m/s
L_1=20m, L_2=30m, Vs_{L1}=700m/s, Vs_{L2}=700m/s
L_1=20m, L_2=30m, Vs_{L1}=800m/s, Vs_{L2}=300m/s
L_1=20m, L_2=30m, Vs_{L1}=800m/s, Vs_{L2}=350m/s
L_1=20m, L_2=30m, Vs_{L1}=800m/s, Vs_{L2}=400m/s
L_1=20m, L_2=30m, Vs_{L1}=800m/s, Vs_{L2}=450m/s
L_1=20m, L_2=30m, Vs_{L1}=800m/s, Vs_{L2}=500m/s
L_1=20m, L_2=30m, Vs_{L1}=800m/s, Vs_{L2}=550m/s
L_1=20m, L_2=30m, Vs_{L1}=800m/s, Vs_{L2}=600m/s
L_1=20m, L_2=30m, Vs_{L1}=800m/s, Vs_{L2}=650m/s
L_1=20m, L_2=30m, Vs_{L1}=800m/s, Vs_{L2}=700m/s
L_1=20m, L_2=30m, Vs_{L1}=800m/s, Vs_{L2}=750m/s
L_1=20m, L_2=30m, Vs_{L1}=800m/s, Vs_{L2}=800m/s
L_1=30m, L_2=20m, Vs_{L1}=400m/s, Vs_{L2}=300m/s
L_1=30m, L_2=20m, Vs_{L1}=400m/s, Vs_{L2}=350m/s
L_1=30m, L_2=20m, Vs_{L1}=400m/s, Vs_{L2}=400m/s
L_1=30m, L_2=20m, Vs_{L1}=500m/s, Vs_{L2}=300m/s
L_1=30m, L_2=20m, Vs_{L1}=500m/s, Vs_{L2}=350m/s
L_1=30m, L_2=20m, Vs_{L1}=500m/s, Vs_{L2}=400m/s
L_1=30m, L_2=20m, Vs_{L1}=500m/s, Vs_{L2}=450m/s
L_1=30m, L_2=20m, Vs_{L1}=500m/s, Vs_{L2}=500m/s
L_1=30m, L_2=20m, Vs_{L1}=600m/s, Vs_{L2}=300m/s
L_1=30m, L_2=20m, Vs_{L1}=600m/s, Vs_{L2}=350m/s
L_1=30m, L_2=20m, Vs_{L1}=600m/s, Vs_{L2}=400m/s
L_1=30m, L_2=20m, Vs_{L1}=600m/s, Vs_{L2}=450m/s
L_1=30m, L_2=20m, Vs_{L1}=600m/s, Vs_{L2}=500m/s
L_1=30m, L_2=20m, Vs_{L1}=600m/s, Vs_{L2}=550m/s
Kramer
A&R
Analytical
$\frac{u_{top}}{s_i}$
freq.[Hz]
0.01
0.10
1
10
100
0
1
2
3
4
5
6

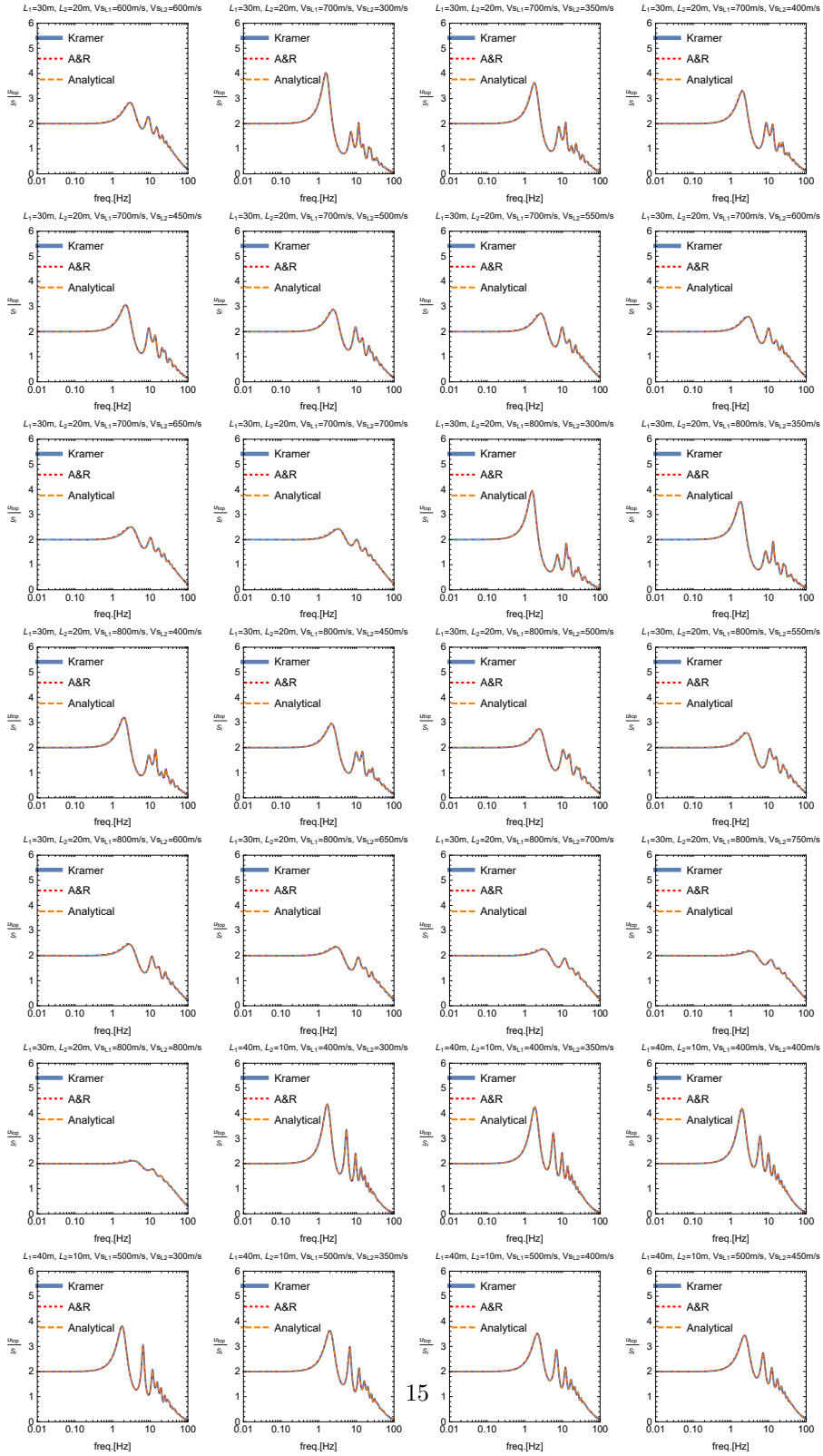
L_1=30m, L_2=20m, Vs_{L1}=600m/s, Vs_{L2}=600m/s
L_1=30m, L_2=20m, Vs_{L1}=700m/s, Vs_{L2}=300m/s
L_1=30m, L_2=20m, Vs_{L1}=700m/s, Vs_{L2}=350m/s
L_1=30m, L_2=20m, Vs_{L1}=700m/s, Vs_{L2}=400m/s
L_1=30m, L_2=20m, Vs_{L1}=700m/s, Vs_{L2}=450m/s
L_1=30m, L_2=20m, Vs_{L1}=700m/s, Vs_{L2}=500m/s
L_1=30m, L_2=20m, Vs_{L1}=700m/s, Vs_{L2}=550m/s
L_1=30m, L_2=20m, Vs_{L1}=700m/s, Vs_{L2}=600m/s
L_1=30m, L_2=20m, Vs_{L1}=700m/s, Vs_{L2}=650m/s
L_1=30m, L_2=20m, Vs_{L1}=700m/s, Vs_{L2}=700m/s
L_1=30m, L_2=20m, Vs_{L1}=800m/s, Vs_{L2}=300m/s
L_1=30m, L_2=20m, Vs_{L1}=800m/s, Vs_{L2}=350m/s
L_1=30m, L_2=20m, Vs_{L1}=800m/s, Vs_{L2}=400m/s
L_1=30m, L_2=20m, Vs_{L1}=800m/s, Vs_{L2}=450m/s
L_1=30m, L_2=20m, Vs_{L1}=800m/s, Vs_{L2}=500m/s
L_1=30m, L_2=20m, Vs_{L1}=800m/s, Vs_{L2}=550m/s
L_1=30m, L_2=20m, Vs_{L1}=800m/s, Vs_{L2}=600m/s
L_1=30m, L_2=20m, Vs_{L1}=800m/s, Vs_{L2}=650m/s
L_1=30m, L_2=20m, Vs_{L1}=800m/s, Vs_{L2}=700m/s
L_1=30m, L_2=20m, Vs_{L1}=800m/s, Vs_{L2}=750m/s
L_1=30m, L_2=20m, Vs_{L1}=800m/s, Vs_{L2}=800m/s
L_1=40m, L_2=10m, Vs_{L1}=400m/s, Vs_{L2}=300m/s
L_1=40m, L_2=10m, Vs_{L1}=400m/s, Vs_{L2}=350m/s
L_1=40m, L_2=10m, Vs_{L1}=400m/s, Vs_{L2}=400m/s
L_1=40m, L_2=10m, Vs_{L1}=500m/s, Vs_{L2}=300m/s
L_1=40m, L_2=10m, Vs_{L1}=500m/s, Vs_{L2}=350m/s
L_1=40m, L_2=10m, Vs_{L1}=500m/s, Vs_{L2}=400m/s
L_1=40m, L_2=10m, Vs_{L1}=500m/s, Vs_{L2}=450m/s
Kramer
A&R
Analytical
$\frac{u_{top}}{s_i}$
freq.[Hz]
0.01
0.10
1
10
100
0
1
2
3
4
5
6

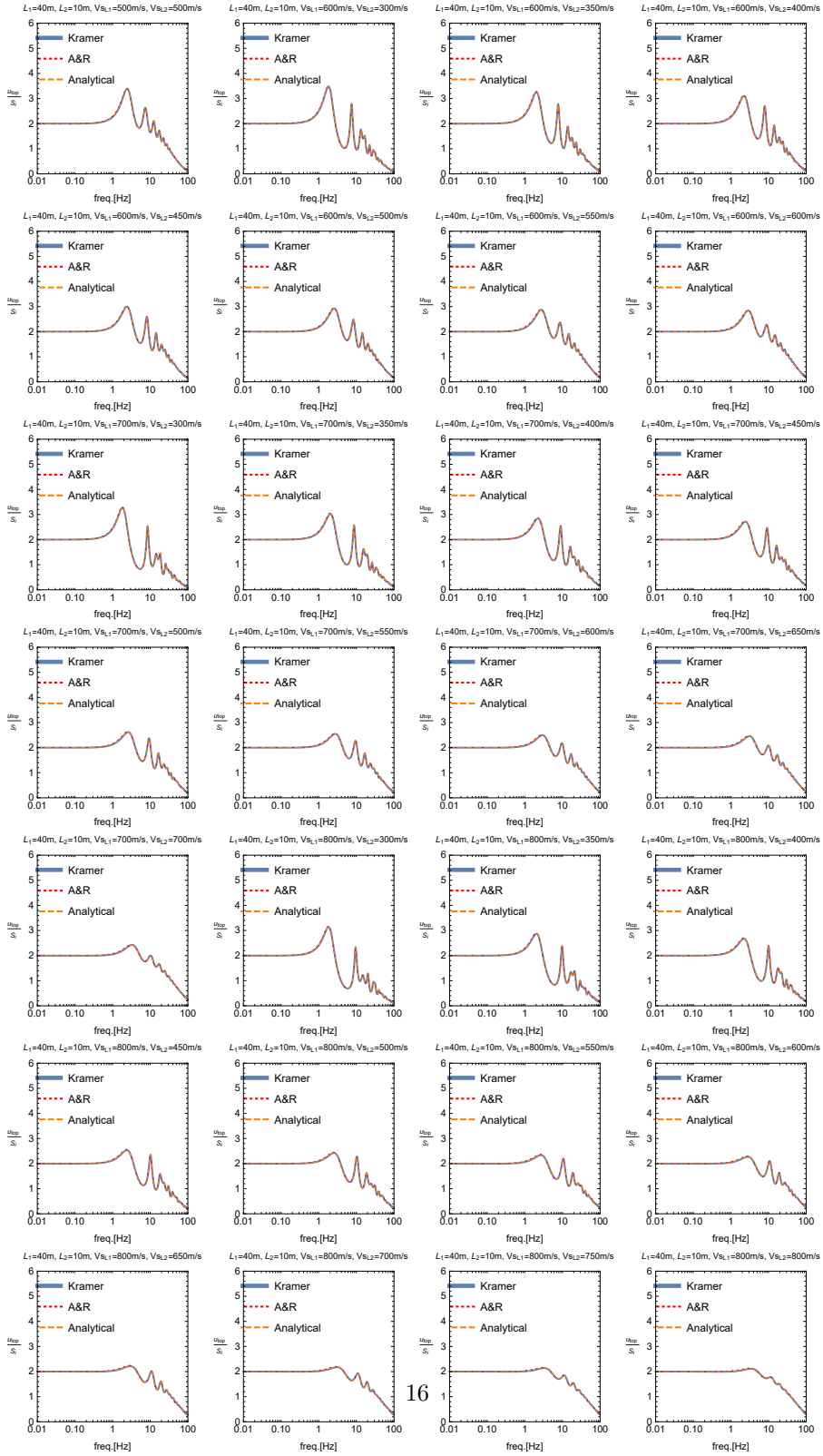
L_1=40m, L_2=10m, Vs_{L1}=500m/s, Vs_{L2}=500m/s
L_1=40m, L_2=10m, Vs_{L1}=600m/s, Vs_{L2}=300m/s
L_1=40m, L_2=10m, Vs_{L1}=600m/s, Vs_{L2}=350m/s
L_1=40m, L_2=10m, Vs_{L1}=600m/s, Vs_{L2}=400m/s
L_1=40m, L_2=10m, Vs_{L1}=600m/s, Vs_{L2}=450m/s
L_1=40m, L_2=10m, Vs_{L1}=600m/s, Vs_{L2}=500m/s
L_1=40m, L_2=10m, Vs_{L1}=600m/s, Vs_{L2}=550m/s
L_1=40m, L_2=10m, Vs_{L1}=600m/s, Vs_{L2}=600m/s
L_1=40m, L_2=10m, Vs_{L1}=700m/s, Vs_{L2}=300m/s
L_1=40m, L_2=10m, Vs_{L1}=700m/s, Vs_{L2}=350m/s
L_1=40m, L_2=10m, Vs_{L1}=700m/s, Vs_{L2}=400m/s
L_1=40m, L_2=10m, Vs_{L1}=700m/s, Vs_{L2}=450m/s
L_1=40m, L_2=10m, Vs_{L1}=700m/s, Vs_{L2}=500m/s
L_1=40m, L_2=10m, Vs_{L1}=700m/s, Vs_{L2}=550m/s
L_1=40m, L_2=10m, Vs_{L1}=700m/s, Vs_{L2}=600m/s
L_1=40m, L_2=10m, Vs_{L1}=700m/s, Vs_{L2}=650m/s
L_1=40m, L_2=10m, Vs_{L1}=700m/s, Vs_{L2}=700m/s
L_1=40m, L_2=10m, Vs_{L1}=800m/s, Vs_{L2}=300m/s
L_1=40m, L_2=10m, Vs_{L1}=800m/s, Vs_{L2}=350m/s
L_1=40m, L_2=10m, Vs_{L1}=800m/s, Vs_{L2}=400m/s
L_1=40m, L_2=10m, Vs_{L1}=800m/s, Vs_{L2}=450m/s
L_1=40m, L_2=10m, Vs_{L1}=800m/s, Vs_{L2}=500m/s
L_1=40m, L_2=10m, Vs_{L1}=800m/s, Vs_{L2}=550m/s
L_1=40m, L_2=10m, Vs_{L1}=800m/s, Vs_{L2}=600m/s
L_1=40m, L_2=10m, Vs_{L1}=800m/s, Vs_{L2}=650m/s
L_1=40m, L_2=10m, Vs_{L1}=800m/s, Vs_{L2}=700m/s
L_1=40m, L_2=10m, Vs_{L1}=800m/s, Vs_{L2}=750m/s
L_1=40m, L_2=10m, Vs_{L1}=800m/s, Vs_{L2}=800m/s
Kramer
A&R
Analytical
$\frac{u_{top}}{s_i}$
freq.[Hz]
0.01
0.10
1
10
100
0
1
2
3
4
5
6